# Surface-Enhanced Raman Spectroscopy of Phosphate Anions: Adsorption on Silver, Gold, and Copper Electrodes

**Gediminas Niaura,* Adolfas K. Gaigalas, and Vincent L. Vilker**

*Biotechnology Division, National Institute of Standards and Technology, Gaithersburg, Maryland 20899*

*Received: January 7, 1997; In Final Form: August 26, 1997*[⊗]

The adsorption of phosphate anions on Ag, Au, and Cu electrodes from $H_2O$ and $D_2O$ solutions has been studied by means of surface-enhanced Raman spectroscopy (SERS). The interpretation of the spectra based on the solution Raman data and frequency shifts upon solution $H_2O/D_2O$ exchange are presented. The prominent band at 1070−1100 $cm^{-1}$, observed from adsorbed $PO_4^{3-}$ and $HPO_4^{2-}$ ions, exhibits downshifts of about 10 $cm^{-1}$ in $D_2O$ solutions and has been assigned to the asymmetric P−O stretching mode. The corresponding asymmetric deformation mode has been assigned to the band located at ∼570 $cm^{-1}$ which shows an upshift of 9−15 $cm^{-1}$ in $D_2O$ solutions. Monodentate surface coordination of the $PO_4^{3-}$ and $HPO_4^{2-}$ ions is proposed. The dependence of the relative intensity of the internal modes on electrode potential was interpreted in terms of the migration of P−O groups from the surface as potential became more negative. Spectroscopic evidence was found for chemisorption of $H_2PO_4^-$ ion on the Cu electrodes, but no such evidence was found in the cases of the Au and Ag electrodes. The adsorbed $H_2PO_4^-$ ion on Cu showed an intense band at ∼907 $cm^{-1}$ which was assigned to the symmetric stretching mode of the P−OH groups, based primarily on the considerable frequency downshift (∼11 $cm^{-1}$) and peak broadening (∼15 $cm^{-1}$) in $D_2O$ solutions. The formation of a P−O−P bond in the adsorbed state on Cu electrodes in acidic solutions is suggested. The force constants derived from experimental metal−oxygen frequencies are compared for the three electrodes, and the following strength order has been estimated: $k$(Cu−O′) > $k$(Au−O′) > $k$(Ag−O′).

## 1. Introduction

The chemisorption of ions can have a significant effect on the overall charge of a solid surface and on the double-layer structure of the interface. This influence of ion coadsorption has been studied in the context of protein adsorption at surfaces and protein bioelectrochemistry at electrodes. The Coulombic interaction of adsorbed ions with the protein's charged surface residues influences extent,[1] conformation, and orientation[2] of the protein on the solid surface. In bioelectrochemistry, Coulombic interactions involving specifically adsorbed anions affect the redox behavior of cytochrome *c* on indium−tin oxide,[3] gold, and silver electrodes.[4] Despite these established effects, and the prevalence of the phosphate buffer system in physiological and biochemical systems, little is understood about the extent or significance of specifically adsorbed phosphate anions at electrodes. In part, this may be due to the complexity that accompanies the existence of multiple protonation states for the phosphate species. Thus, we undertook a comparative SERS investigation of the adsorption of the phosphate anions on silver, copper, and gold electrodes. These results enable us to identify the influence of the nature of the metal electrode, through the adsorption of phosphate species, in our related studies on heterogeneous electron transfer to proteins.[5]

SERS can provide in situ information about the chemical identity of the adsorbed species, protonation/deprotonation state, molecular structure, and orientation of adsorbates at surfaces.[6,7] The vibrational spectra of adsorbed species can be recorded over a wide frequency range (100−4000 $cm^{-1}$) including the particularly interesting metal−adsorbate modes[8] below 400 $cm^{-1}$. Surface IR spectroscopy and SERS have been used to characterize surface-bound phosphate ions on Ag colloids[9,10] and on Ag, Au, and Pt electrodes.[11−16] Analysis of the SER spectra obtained in these electrode studies has led to a better understanding of the relationship between interfacial pH and the protonation state of the adsorbed phosphate anions. However, controversy still remains about the interpretation of the observed spectra.[9−11] We have not found reports of Raman studies for adsorbed phosphate species on Au and Cu electrodes.

## 2. Experimental Section

Phosphate solutions were prepared from reagent grade $Na_2HPO_4$, $NaH_2PO_4$, NaOH, $HClO_4$, and distilled/deionized water. $D_2O$ was obtained from ISOTEC Inc. (Catalog. No. 82-70046).[17]

Electrochemical and surface Raman measurements were performed in a cylindrical spectroelectrochemical cell with three electrodes. The counter electrode was a Pt wire. Polycrystalline rods (Aldrich Chemical Co.) of Ag (99.99% grade), Au (99.99% grade), and Cu (99.999% grade) pressed into Teflon sleeves served as the working electrodes. The potential ($E$) of the working electrode was measured versus a saturated Ag/AgCl reference electrode. All potentials were converted and are presented versus standard hydrogen electrode (SHE). Prior to use, the solutions were deoxygenated by bubbling Ar for about 40 min.

The surface of a working electrode was placed ∼2 mm from the spectroelectrochemical cell window. The excitation source was the 632.8 nm line from a He−Ne laser (∼10 mW power at the sample). The laser beam was incident on the surface at an angle of ∼60° with respect to the surface normal and focused to a ∼1 $mm^2$ spot. The experiments were performed in 90° geometry. The laser plasma lines were attenuated by means of an interference filter. The holographic laser-line filter was put in front of the monochromator in order to eliminate Rayleigh scattering from the electrode. The Raman scattering light was analyzed with the SPEX 14018 double monochromator converted to single use with 1800 lines/mm grating and connected

* Corresponding author. Fax (301) 975 5449; e-mail vincent.vilker@nist.gov.

[⊗] Abstract published in *Advance ACS Abstracts,* October 1, 1997.

S1089-5647(97)00097-7 CCC: $14.00 

**TABLE 1: Calculated Concentrations[a] of the Phosphate Species and $OH^-$ Ions**

| solution | pH | $[PO_4^{3-}]$ | $[HPO_4^{2-}]$ | $[H_2PO_4^-]$ | $[H_3PO_4]$ | $[OH^-]$ |
|---|---|---|---|---|---|---|
| I. 1 M NaOH + 0.067 M $Na_2HPO_4$ | 14.0 | $6.50 \times 10^{-2}$ | $2 \times 10^{-3}$ | $10^{-10}$ | $10^{-22}$ | $9.4 \times 10^{-1}$ |
| II. 0.1 M NaOH + 0.067 M $Na_2HPO_4$ | 12.47 | $5.9 \times 10^{-2}$ | $8.5 \times 10^{-3}$ | $1.6 \times 10^{-8}$ | $10^{-19}$ | $4.2 \times 10^{-2}$ |
| III. 0.067 M $Na_2HPO_4$ | 9.31 | $2.8 \times 10^{-4}$ | $6.7 \times 10^{-2}$ | $2.0 \times 10^{-4}$ | $10^{-11}$ | $2.8 \times 10^{-5}$ |
| IV. 0.067 M $NaH_2PO_4$ | 4.22 | $10^{-12}$ | $1.4 \times 10^{-4}$ | $6.7 \times 10^{-2}$ | $4.6 \times 10^{-4}$ | $10^{-10}$ |
| V. 0.1 M $HClO_4$ + 0.067 M $NaH_2PO_4$ | 1.38 | $10^{-18}$ | $9 \times 10^{-8}$ | $2.3 \times 10^{-2}$ | $4.4 \times 10^{-2}$ | $10^{-13}$ |

[a] The concentrations of anionic species were calculated using published p$K_a$ values.[20] The activity coefficients for solutions II−V were calculated by the Davies equation[21] and for solution I by the Robinson−Guggenheim−Bates modified by the Debye−Huckel equation.[20]

**TABLE 2: Frequencies ($\nu$, $cm^{-1}$), Full Widths at Half-Maximum (fwhm, $cm^{-1}$), and Frequency Shifts upon Solution $H_2O/D_2O$ Exchange ($\Delta$, $cm^{-1}$ ) of the Phosphate Raman Bands from Aqueous Solutions Prepared with $H_2O$ or $D_2O$ (0.067 M Total Phosphate Concentration)**

| $H_2O$ | | $D_2O$ | | | | |
|---|---|---|---|---|---|---|
| $\nu$ | fwhm | $\nu$ | fwhm | $\Delta$ | assign[a] | sym mode |
| | | | $PO_4^{3-}$, from Solution I | | | |
| 415.5 | 49 | 415.1 | 67 | $0 \pm 2$ (w) | $\delta_s(PO_4)$ | E |
| 553.9 | 52 | 560.1 | 57 | $6 \pm 2$ (w) | $\delta_{as}(PO_4)$ | $F_2$ |
| 936.3 | 28.7 | 935.3 | 13.1 | $-1 \pm 0.4$ (vs) | $\nu_s(PO_4)$ | $A_1$ |
| 1013 | 57 | 1005 | 51 | $-8 \pm 2$ (w) | $\nu_{as}(PO_4)$ | $F_2$ |
| | | | $HPO_4^{2-}$, from Solution III | | | |
| 855.1 | 51 | 832.7 | 40 | $-22 \pm 2$ (m) | $\nu$[P−(OH)] | $A_1$ |
| 989.6 | 16.8 | 987.3 | 12.1 | $-2.3 \pm 0.4$ (vs) | $\nu_s(PO_3)$ | $A_1$ |
| 1083.3 | 36 | 1087.8 | 60 | $4 \pm 2$ (w) | $\nu_{as}(PO_3)$ | E |
| | | | $H_2PO_4^-$, from Solution IV | | | |
| 876.8 | 23.1 | 859.3 | 39.8 | $-17.5 \pm 0.4$ (m) | $\nu_s$[P−$(OH)_2$] | $A_1$ |
| 1076.8 | 23.6 | 1083.7 | 20.5 | $6.9 \pm 0.4$ (s) | $\nu_s(PO_2)$ | $A_1$ |

[a] Assignments based on data from refs 22 and 23. Abbreviations: $\nu$ = stretching; $\delta$ = deformation; s = symmetric; as = asymmetric; w = weak; m = middle; s = strong; vs = very strong; $\Delta = \nu(D_2O) - \nu(H_2O)$.

to a SPEX Spectrum One charge coupled detector (CCD). The spectral slit width was $s = 4$ $cm^{-1}$; overall integration time was 10−30 s. The overlapping bands were deconvoluted into a sum of Gaussian and Lorentzian shapes using Grams/386 (Galactic industries Co.) software. The Raman frequencies were calibrated using the laser plasma lines. Spectroelectrochemical experiments were carried out using EG & G PAR Model 173 potentiostat with PAR Model 175 signal generator.

The SERS active electrodes were prepared as follows:

(a) Ag electrodes were electrochemically roughened in the deaerated 1 M $NaClO_4$ solution by cycling three times from −0.3 to 0.8 V (sweep rate 100 mV/s), with holds of 30 s at the negative potential and 10 s at the positive potential.

(b) Au electrodes were electrochemically roughened in 0.1 M NaCl solution by a slightly modified procedure from that described in ref 18. The electrode activation was carried out by cycling six times from −0.1 to 1.3 V (sweep rate 100 mV/s), with holds of 10 s at the positive potential and 30 s at the negative potential.

(c) Cu electrodes were activated as described in ref 19. Briefly, a Cu layer (∼10 $\mu$m) was electrodeposited on a polished Cu electrode from an acid copper plating bath. Next, an additional Cu layer was electrodeposited from 0.02 M $CuSO_4$ (pH 4.5) solution at −0.3 V (electrodeposition time was 120 s); then the electrode was immersed in the deoxygenated 0.5 M $H_2SO_4$ + 0.5 M $Na_2SO_4$ solution and held at open-circuit potential for 90 min. Finally, the electrode was rinsed with deoxygenated water and transferred to the spectroelectrochemical cell.

## 3. Results

To investigate adsorption properties of phosphate anions, we studied five solutions (identified as I−V), each with the same total phosphate concentration but with different relative concentrations of phosphate anionic species. Table 1 summarizes the estimated concentration of each phosphate species ($PO_4^{3-}$, $HPO_4^{2-}$, $H_2PO_4^-$, and $H_3PO_4$ ) in the five solutions. Solution Raman spectra in $H_2O$ and $D_2O$ were obtained and interpreted prior to undertaking the SERS studies on metal electrode surfaces. From the set of Raman-active modes, only those that were clearly resolvable in both $H_2O$ and $D_2O$ were selected for interpretation.

The concentration of the $OH^-$ ions varies in these systems and is also shown in Table 1. In general, three surface processes need to be considered in these systems: (a) adsorption of phosphate anions, (b) adsorption of $OH^-$ ions, and (c) surface oxide formation. Hydroxide ions can compete for adsorption sites with the phosphate anionic species while formation of surface oxides can modify their adsorption/desorption behavior. Cyclic voltammetry is used along with SERS in order to determine surface oxide formation. Features of the SER spectra arising from surface oxides and surface $OH^-$ ions are interpreted.

**3.1. Solution Spectra.** Assignments of modes rely on previous vibrational spectra measurements made using infrared[22] and Raman spectroscopy.[23] The frequencies of the Raman bands, widths (quantitatively defined as "full width at half -maximum peak height" or fwhm), and frequency shifts upon solution $H_2O/D_2O$ exchange ($\Delta$) are summarized in Table 2. The fwhm and frequency shift measurements are useful for interpreting environmental influences (e.g., hydrogen bonding to solvent) on the vibrational spectra.

In aqueous solutions, $PO_4^{3-}$ ion has tetrahedral symmetry ($T_d$), and the vibrational spectrum is made up of four modes. Displacements of atoms during stretching vibrations are shown in Figure 1. The most intense band is related to the totally symmetric ($A_1$) stretching vibration $\nu_s(PO_4)$. Considerably lower intensity bands are associated with the triple-degenerate asymmetric ($F_2$) stretching mode $\nu_{as}(PO_4)$, the triple-degenerate asymmetric deformation mode $\delta_{as}(PO_4)$, and the double-degenerate symmetric (E) deformation mode $\delta_s(PO_4)$. The most interesting observation is the clear shift in the frequencies of the asymmetric stretching mode, $\nu_{as}(PO_4)$, and the asymmetric

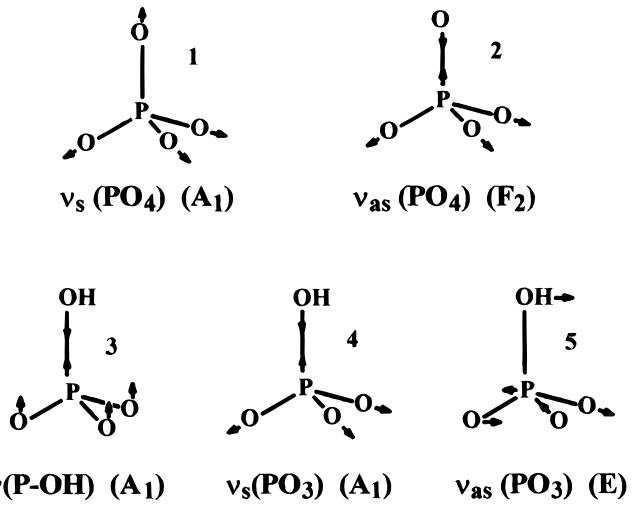


**Figure 1.** Normal-mode stretching vibrations for $PO_4^{3-}$ (1, 2) and $HPO_4^{2-}$ (3−5) ions (from ref 24).

deformation mode, $\delta_{as}(PO_4)$, upon solution $H_2O/D_2O$ exchange. The totally symmetric mode, $\nu_s(PO_4)$, is also affected by $H_2O/D_2O$ exchange. In this case, fwhm is the most sensitive parameter; fwhm decreased in $D_2O$ to about half the value seen in $H_2O$. This may be due to differences in hydrogen-bonding strength between phosphate anions and water molecules in $H_2O$ and $D_2O$ solutions.[22]

For solutions in which the dominant ionic species is $HPO_4^{2-}$, three stretching modes of the vibrational spectra were observed. The bonding of hydrogen ion to $PO_4^{3-}$ results in reduced symmetry in the $HPO_4^{2-}$ ion. The OH group is treated as a point mass, and the symmetry is modeled as $C_{3v}$,[22] where the degenerate asymmetric stretching mode ($F_2$) splits into the symmetric and asymmetric stretches of the $PO_3$ group (Figure 1). The stretching vibration of the P−(OH) bond can be easily recognized by the large negative frequency shift upon solution $H_2O/D_2O$ exchange.[22] Detectable frequency downshift and band narrowing also were observed for the symmetric $\nu_s(PO_3)$ mode in $D_2O$ solutions. The frequency of the $\nu_{as}(PO_3)$ mode upshifted in $D_2O$ solutions, which is opposite to the direction of the shift that was seen for the $\nu_{as}(PO_4)$ mode in $PO_4^{3-}$. This upward shift is related to coupling of the $\nu_{as}(PO_3)$ vibration with the P−O−H in-plane deformation.[22]

Bonding of two hydrogen ions to the $PO_4^{3-}$ ion further reduces symmetry to $C_{2v}$ in the $H_2PO_4^-$ ion where the OH groups are treated as a point masses.[22] Again, a large negative frequency shift upon solution $H_2O/D_2O$ exchange is associated with the symmetric stretching vibrations of the P−(OH) bonds.[22] This mode also became broader in $D_2O$. Coupling of the $\nu_s(PO_2)$ mode with P−O−H in-plane deformation is responsible for an upward shift of the $\nu_s(PO_2)$ frequency in $D_2O$ solutions.

**3.2. Silver Electrode Surface Spectra.** Strong spectra have been obtained only in solutions I, II, and III which contain predominantly $HPO_4^{2-}$ and $PO_4^{3-}$ species. No SER spectra were detected in solutions IV and V over a wide potential range (0.3 to −0.6 V). This indicates absence or minimal extent of $H_2PO_4^-$ or $H_3PO_4$ species adsorption on the silver electrode.

Figure 2 shows the potential dependence of the SER spectra in solutions II and III. The cyclic voltammograms (CV) (see inserts) show that no oxidation or reduction processes took place in the potential region of interest. Surface oxide formation was not indicated in either CV or SERS data for solutions II or III. These observations suggest that the influence of potential on the SER spectra is related to changes in adsorption of phosphate species on the electrode surface. In both solutions II and III,

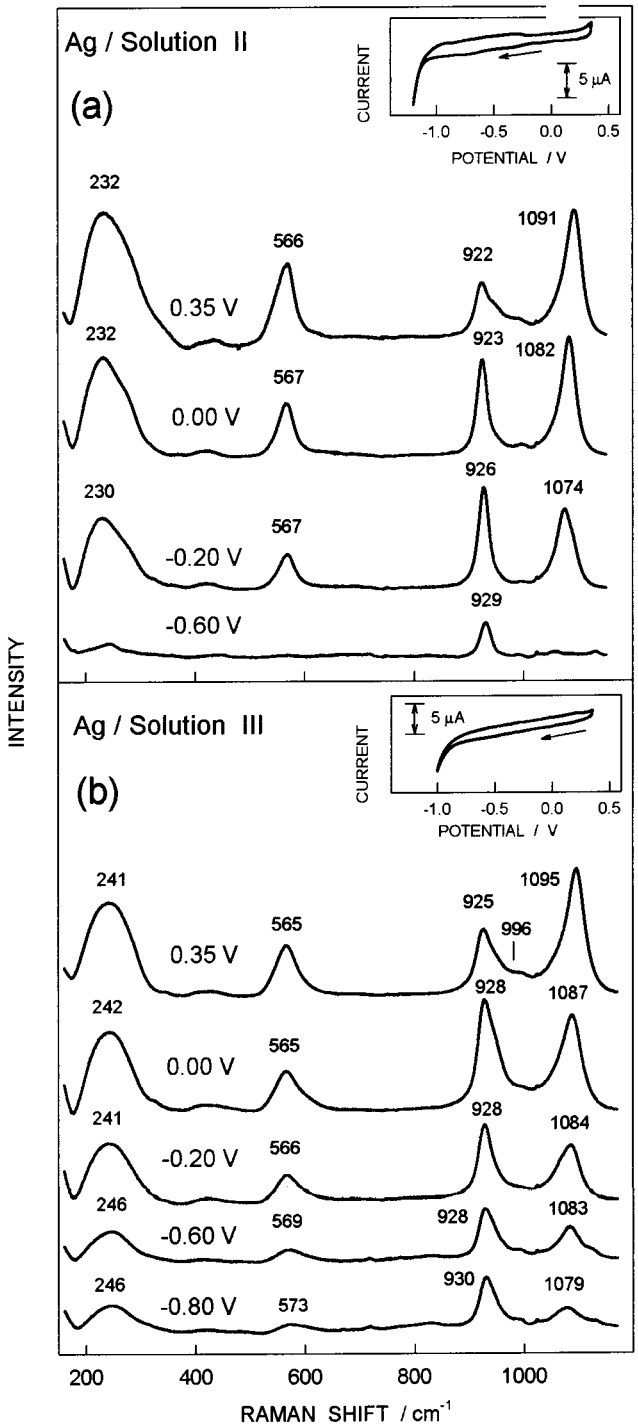


**Figure 2.** Dependence of the SER spectra on Ag electrode potential: (a) solution II (0.1 M NaOH + 0.067 M $Na_2HPO_4$); (b) solution III (0.067 M $Na_2HPO_4$). Inserts show cyclic voltammograms covering same potential range. Potential sweep rate, 20 mV/s.

the frequency shifted downward with decreasing potential for the bands in the 1070−1095 cm$^{-1}$ range. For bands in the range 920−930 cm$^{-1}$, the frequency shifted slightly upward with decreasing potential. In the ranges 230−240 and 560−570 cm$^{-1}$, frequency shifts due to potential changes were negligible. The intensity ratio $I_{922-930}/I_{1070-1095}$ increased as potential decreased. Only solution III gave a clear spectrum below potentials more negative than about −0.6 V where the band located at ∼1070−1090 cm$^{-1}$ completely disappeared in solution II.

Comparison of SER spectra in different solutions at the same electrode potential, and the influence of the solution $H_2O/D_2O$ exchange on the spectra, are presented in Figure 3. Spectra

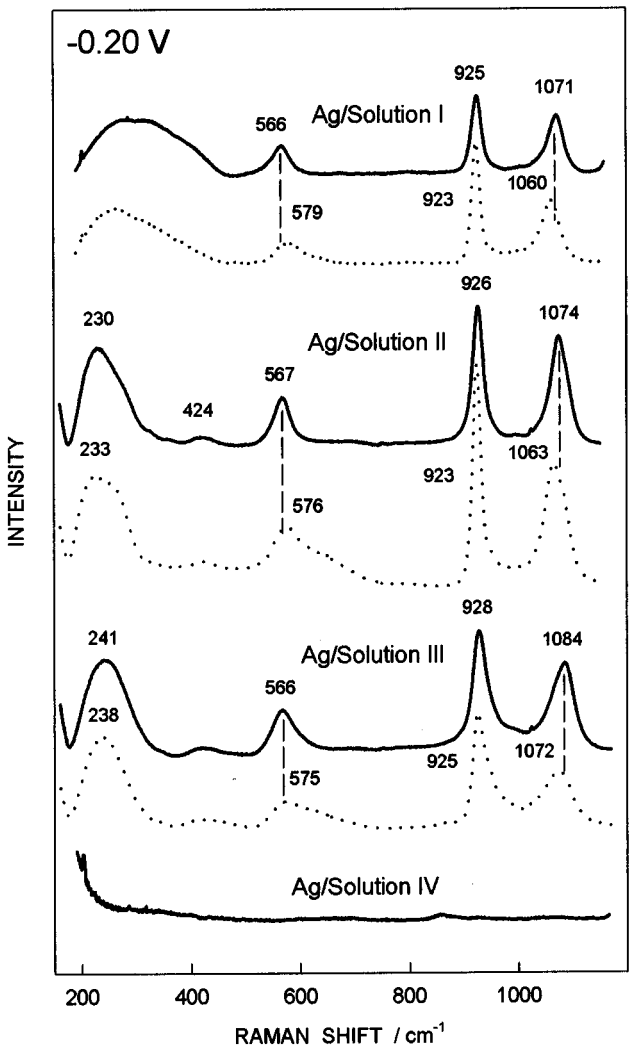


**Figure 3.** SER spectra of adsorbed phosphate anions on Ag electrode at $E = -0.20$ V from different solutions prepared with $H_2O$ (solid line) and $D_2O$ (dotted line).

obtained in solutions I and II are very similar in the range between 400 and 1200 $cm^{-1}$, indicating the same adsorbed species in both cases. The extended breadth of the band in the low-frequency region (200−400 $cm^{-1}$) of solution I is most likely related to interactions of $OH^-$ with the silver electrode. The spectrum of solution III differs from the spectrum of solution II in that the highest frequency mode is shifted from 1074 to 1084 $cm^{-1}$, the low-frequency mode is shifted from 230 to 241 $cm^{-1}$, and fwhm is increased for bands located in the region 900−1100 $cm^{-1}$. These differences are most likely due to the adsorption of the different anions (e.g., $PO_4^{3-}$ and $HPO_4^{2-}$) at the same potential and due to the effect of hydrogen bonding between adsorbed anions or between anions and water.

Further details about the nature of the adsorbed species and the effect of hydrogen bonding can be obtained from solution $H_2O/D_2O$ isotopic-exchange experiments. The $D_2O$ SER spectra of adsorbed phosphate anions (Figure 3) show that (a) frequency shifts upon solution $H_2O/D_2O$ exchange $\Delta$ ($\Delta = \nu(D_2O) - \nu(H_2O)$) were not uniform—they were negative 9−12 $cm^{-1}$ for the highest frequency bands at 1070−1090 $cm^{-1}$, nearly absent for the most intense band at 923−926 $cm^{-1}$, and positive 9−13 $cm^{-1}$ for the bands located in the region of 566 $cm^{-1}$; (b) fwhm of the band around 926 $cm^{-1}$ decreased by ~5 $cm^{-1}$, while the fwhm of the bands located at 1070 and 567 $cm^{-1}$ increased; (c) the band at 576 $cm^{-1}$ was apparently overlapped by a new band around 660 $cm^{-1}$. An interpretation of these solution $H_2O/D_2O$ substitution effects is given later.

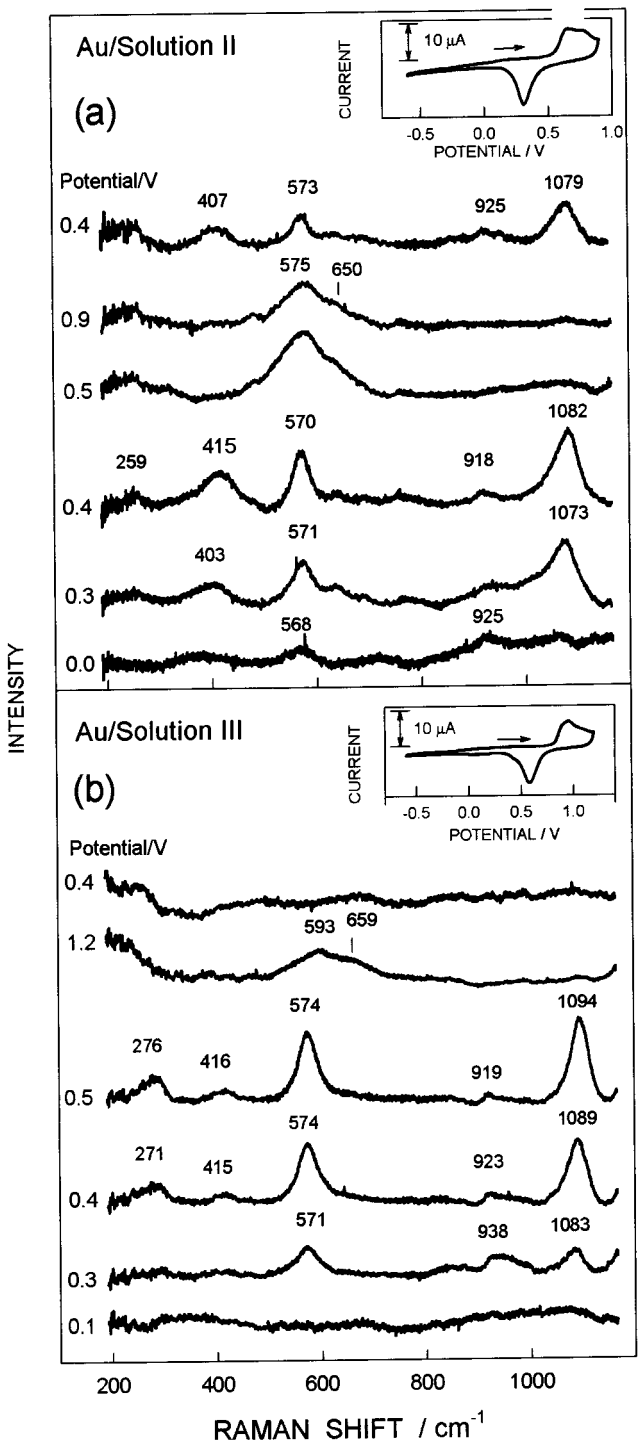


**Figure 4.** Dependence of the SER spectra on Au electrode potential: (a) solution II (0.1 M NaOH + 0.067 M $Na_2HPO_4$); (b) solution III (0.067 M $Na_2HPO_4$). Inserts show cyclic voltammograms covering same potential range. Potential sweep rate, 50 mV/s.

**3.3. Gold Electrode Surface Spectra.** SER spectra on Au electrodes were observed only in solutions II and III (Figures 4 and 5) where $PO_4^{3-}$ and $HPO_4^{2-}$ are the dominant solution anions and $OH^-$ is not in large excess. The most pronounced bands are located at 570−574 and 1080−1090 $cm^{-1}$.

The cyclic voltammogram and the corresponding potential-dependent SER spectra are shown in Figure 4. When an activated Au electrode was dipped into solution II at $E = 0.40$ V, the first spectrum (from the top) of Figure 4a was observed. As electrode potential was made more positive, the CV response indicated formation of surface oxides at $E \sim 0.6-0.9$ V. The spectrum at 0.9 V of Figure 4a indicates that bands around 1080

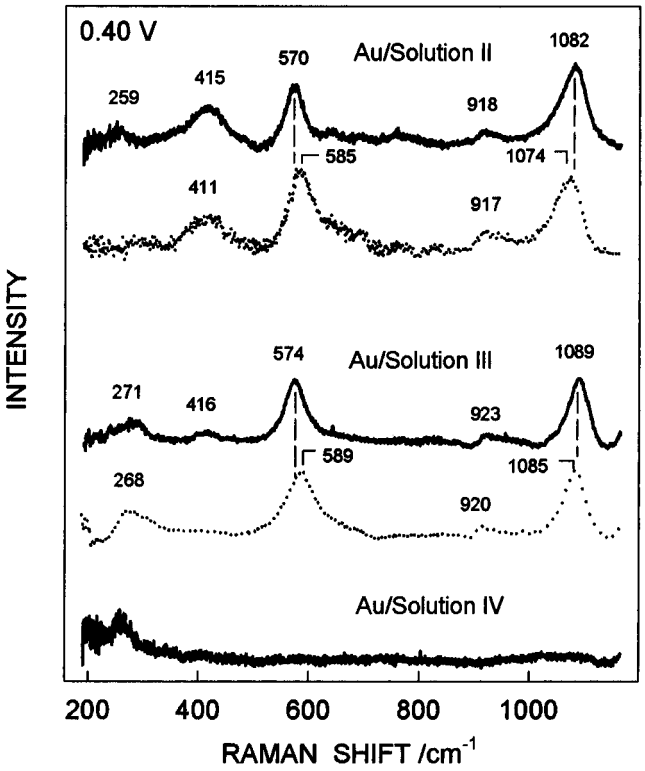


**Figure 5.** SER spectra of adsorbed phosphate anions on Au electrode at $E = 0.40$ V from different solutions prepared with $H_2O$ (solid line) and $D_2O$ (dotted line). Electrodes were subjected to oxide formation and reduction in situ before spectra were taken (see Figure 4).

$cm^{-1}$ disappeared while there was enhancement of a broad feature located around 575 $cm^{-1}$. (Deconvolution into the Gaussian components yields two bands: 575 (fwhm = 82 $cm^{-1}$) and 650 $cm^{-1}$ (fwhm = 93 $cm^{-1}$).) As electrode potential was swept back to less positive values, peak positions remained unchanged (Figure 4a, spectrum at 0.5 V). When the surface oxide reduction potential of 0.4 V was reached, as indicated by the CV cathodic peak (Figure 4a, spectrum at 0.4 V), the prominent SERS bands at 415 and 1082 $cm^{-1}$ appeared, and the broad band around 570−575 $cm^{-1}$ was narrowed. This is adopted as our characteristic phosphate anion adsorption spectra. The intensity of these bands was significantly attenuated as electrode potential was taken to more negative values.

When an activated Au electrode was immersed in the less alkaline solution III at $E = 0.40$ V, the first spectrum (from the top) of Figure 4b was observed. This spectrum is relatively featureless compared to its counterpart solution II spectrum of Figure 4a. As potential was swept to more positive values, the voltammogram again indicated formation of surface oxides, probably corresponding to the broad band around 600 $cm^{-1}$ in the SER spectrum (Figure 4b, spectrum at 1.2 V). The spectrum at 0.5 V of Figure 4b showed the return of the characteristic adsorbed phosphate anion bands that were seen in solution II at about 0.4 V. The prominent bands located at ∼1094 and 574 $cm^{-1}$ appeared as well as the lower intensity bands at ∼276, 416, and ∼920 $cm^{-1}$. The intensity of all these bands rapidly decreased as potential was swept to less positive values.

The SERS bands show clear frequency shifts upon solution $H_2O/D_2O$ exchange (Figure 5). The 570−580 $cm^{-1}$ bands were upshifted by the exchange, and the 1080−1090 $cm^{-1}$ bands were downshifted. The band located around 415 $cm^{-1}$ is more intense in solution II compared with solution III. Spectra from solution I (not shown) also showed broad features in the region 400−430 $cm^{-1}$ at all potentials more positive than −0.30 V. Later, we will indicate evidence that suggests that in this region there are contributions from vibrations of both adsorbed phosphate and $OH^-$ ions and that no SERS bands from adsorbed phosphate anions in solution I were found due to the high $OH^-$ concentration.

**3.4. Copper Electrode Surface Spectra.** In solution I, only SERS features associated with copper oxide and adsorbed $OH^-$ species were observed over the wide potential region 0.30 to −1.40 V. The spectra were similar to the spectrum at −0.2 V of Figure 6a for a Cu electrode immersed in solution II. The potential dependence of the SER spectra from Cu electrodes in solutions II, III, IV, and V, and the corresponding CV responses, are presented in Figure 6. In solution II, the pair of anodic and cathodic peaks located in the potential region −0.1 to −0.3 V (Figure 6a, CV insert) are related with the formation and reduction of the Cu(I) species (solid $Cu_2O$ and soluble Cu(I)), as has been established by voltammetric, X-ray diffraction, and ellipsometric investigations of others.[25−28] In the SER spectra, only features related with Cu oxide and adsorbed $OH^-$ ions were observed at electrode potentials that were more positive than about −0.4 V (Figure 6a). Several broad peaks appear in the region of 400−600 $cm^{-1}$ in the spectra obtained at −0.2 V and at potentials more positive than the voltammetric reduction peak. Deconvolution of these peaks into Gaussian components yields four bands located at 433, 529, 580, and 618 $cm^{-1}$. For more negative electrode potential, weak broad bands at 302 and 607 $cm^{-1}$ and sharper bands at 930 and 1103 $cm^{-1}$ were observed. These features will be ascribed later to adsorbed phosphate anions.

In solution III, the Figure 6b insert shows that the reduction process has shifted to more positive potential relative to solution II (Figure 6a, insert) in response to the decreased hydroxide ion concentration. In general, the same SERS features were observed as in the spectra from solution II. It is noteworthy that the low-frequency band in solution III has shifted to higher frequency (321 $cm^{-1}$) compared with solution II (302 $cm^{-1}$). The most pronounced band located at around 933 $cm^{-1}$ in the spectra from both solutions has been retained even at the very negative potential of −1.20 V.

In the acidic solutions IV and V, Figure 6, c and d, respectively, features associated with copper oxides were not found in either the voltammograms or the SER spectra. However, unlike the SER spectra with Au and Ag electrodes, strong SERS features were seen for these Cu electrodes in response to the high concentrations in solutions IV and V of $H_2PO_4^-$ and $H_3PO_4$. The most intense SERS bands were around 910 and 908 $cm^{-1}$ for solutions IV and V, respectively. These bands decreased in frequency and intensity as electrode potential was made more negative and disappeared below about −0.5 V. The spectral contour in the 850−1150 $cm^{-1}$ region was deconvoluted into Gaussian components that led to the band designations shown in Figure 6c,d. The band at 975 $cm^{-1}$ in Figure 6c appeared to be upshifted in frequency as the electrode potential became more negative.

The effects of $H_2O/D_2O$ exchange are shown in Figure 7. The high-frequency modes in the region 800−1150 $cm^{-1}$ were sensitive to $H_2O/D_2O$ exchange. In solutions II and III, the mode located at 1103−1105 $cm^{-1}$ showed a large downshift ($\Delta = -(8-12) \pm 3$ $cm^{-1}$) while the mode at 930−932 $cm^{-1}$ showed a smaller shift ($\Delta = -(3-4) \pm 2$ $cm^{-1}$) and a decrease in bandwidth (solution II, fwhm decreased from 31 $cm^{-1}$ in $H_2O$ to 25 $cm^{-1}$ in $D_2O$). In the more acidic solutions IV and V (Figure 7), the SER spectra are seen to be more complex, and several bands were sensitive to the solution $H_2O/D_2O$ exchange. The most intense band in solution IV located at 908 $cm^{-1}$ showed a clear downshift upon solution $H_2O/D_2O$

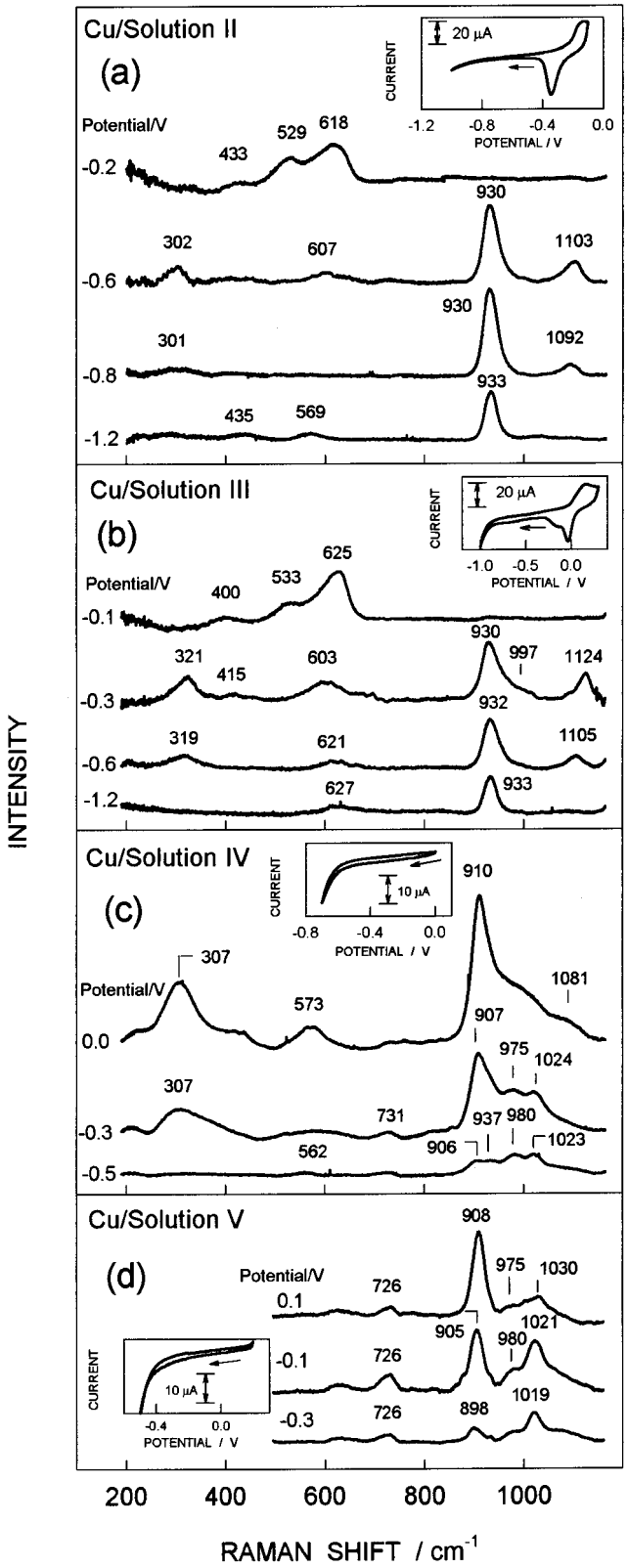


**Figure 6.** Dependence of the SER spectra on Cu electrode potential: (a) solution II (0.1 M NaOH + 0.067 M $Na_2HPO_4$); (b) solution III (0.067 M $Na_2HPO_4$); (c) solution IV (0.067 M $NaH_2PO_4$); (d) solution V (0.1 M $HClO_4$ + 0.067 M $NaH_2PO_4$). Inserts show cyclic voltammograms covering same potential range. Potential sweep rate, 50 mV/s.

exchange, $\Delta = -11 \pm 3$ cm$^{-1}$, and an increase in bandwidth (fwhm increased from 35 cm$^{-1}$ in $H_2O$ to 47 cm$^{-1}$ in $D_2O$, at $E = -0.2$ V). The mode located at 971 cm$^{-1}$ shifted in the opposite direction, $\Delta = 10 \pm 7$ cm$^{-1}$, although low intensity and band overlap caused large uncertainty in the $\Delta$ determination. Other bands at 1022 cm$^{-1}$ ($\Delta = 0 \pm 4$ cm$^{-1}$) and 726 cm$^{-1}$ ($\Delta = -1 \pm 4$ cm$^{-1}$) showed no shifts within experimental error. In solution V, only the band at 902 cm$^{-1}$ showed a clear downshift upon solution $H_2O/D_2O$ exchange ($\Delta = -15 \pm 5$ cm$^{-1}$). This band also increased in width in $D_2O$ solution (fwhm increased from 30 cm$^{-1}$ in $H_2O$ to 45 cm$^{-1}$ in $D_2O$, at $E = -0.2$ V). These frequency shift comparisons for solutions IV and V suggest that the 908 and 902 cm$^{-1}$ bands have the same origin, as do the bands at 1022 and 1020 cm$^{-1}$.

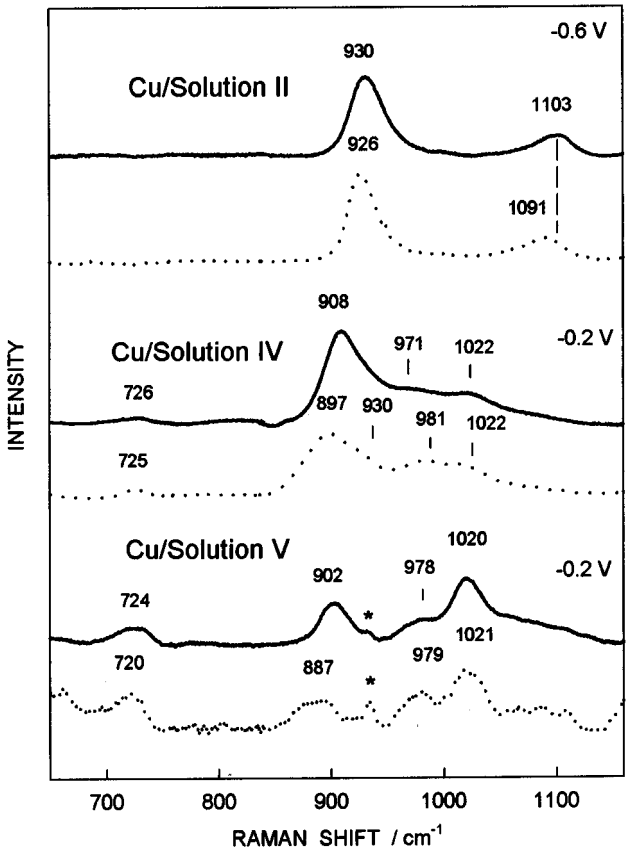


**Figure 7.** SER spectra from adsorbed phosphate anions on Cu electrode from different solutions prepared with $H_2O$ (solid line) and $D_2O$ (dotted line). Asterisk denotes the band from solution-phase $ClO_4^-$ ion.

## 4. Discussion

Three surface species were observed in our SER spectra: surface oxides, adsorbed hydroxide ions, and adsorbed phosphate anions. In the first part of the discussion, features related to the surface oxides and hydroxide ions are identified using relevant existing literature reports. The emphasis will be on the discrimination between these two species, oxides and hydroxides, using our observed frequency shift data derived from solution $H_2O/D_2O$ exchange. Spectral features associated with surface oxides will not display a Raman frequency shift when $D_2O$ is substituted for $H_2O$, whereas features associated with adsorbed hydroxide ions will display such frequency shifts. The interpretation of the spectra associated with adsorbed phosphate species is discussed next. Interpretation and vibrational band assignments are closely related to adsorption geometry, and these two matters are discussed together. Evidence of the formation of polyphosphate species on Cu electrode surfaces in acidic solutions will be presented. Finally, the adsorption properties of phosphate species on Ag, Au, and Cu electrodes will be compared.

**4.1. Spectra Interpretation: Oxides and Adsorbed Hydroxide Ions.** Formation of surface oxide species was observed

only on Au and Cu electrodes. In the case of Au in alkaline solution II, at potentials where cyclic voltammetry indicated an oxidation process (see Figure 4a, spectra obtained at 0.9 and 0.5 V), the broad feature at 500−700 $cm^{-1}$ has been deconvoluted into two components located at 575 and 650 $cm^{-1}$. The band at 575 $cm^{-1}$ showed a negative frequency shift upon substitution of $H_2O$ by $D_2O$, $\Delta = -10 \pm 5$ $cm^{-1}$ (data not shown). This band has been assigned as an Au−OH surface compound, as was proposed earlier.[29] The obscured peak at 650 $cm^{-1}$ did not display a clear response upon $D_2O$ substitution. This band is tentatively attributed to the Au−O vibration, based largely on the previous characterization of gold oxide, $Au_2O_3$, using high-resolution electron energy loss spectroscopy (HREELS), Auger, and X-ray photoelectron spectroscopies performed in ultrahigh vacuum.[30] These two bands also appear in the spectra from the less alkaline solution III (Figure 4b, spectrum at 1.2 V), although at slightly higher frequencies. Frequency shift responses due to deuterated solvent exchange were the same as observed in solution II. When electrode potential was cycled toward lower values where reduction processes were observed, spectra in solutions II and III showed a loss of the broad feature around 500−700 $cm^{-1}$ and an emergence of peaks at 400−430, 570−575, and 1070−1095 $cm^{-1}$. We will discuss later why the origin of most of these peaks is due to adsorbed phosphate ion vibrations but indicate now that there is also a surface hydroxide component associated with the low-frequency peak around 400−430 $cm^{-1}$ in the spectra of Figure 4a. We identify this peak as a hydroxide-associated vibration for several reasons: (i) a similar feature was observed in the SERS studies of Desilvestro and Weaver,[29] (ii) the intensity of this peak increased as solution alkalinity increased, and (iii) a frequency shift upon solution $H_2O/D_2O$ exchange was observed for this peak, $\Delta = -7 \pm 3$ $cm^{-1}$ (data not shown). Therefore, in the high $OH^-$ concentration of solutions I (data not shown) and II, this band is assigned to stretching vibration, $\nu$(Au−$OH^-$), of specifically adsorbed $OH^-$ anions. At more negative potentials and in less alkaline solutions (Figure 4b), this peak is probably a mix of hydroxide and phosphate ion contributions. Competition between $OH^-$ and phosphate anions is thought to be the reason no SER spectrum from phosphate species was observed in our solution I.

In the case of Cu electrodes, oxide-associated features were observed in the alkaline solutions I (data not shown), II, and III. The bands located at 529 and 618 $cm^{-1}$ in the spectrum at −0.2 V of Figure 6a and at 533 and 625 $cm^{-1}$ in the spectrum at −0.1 V of Figure 6b showed no frequency shifts upon solution $H_2O/D_2O$ exchange (experimental error, ±5 $cm^{-1}$). Therefore, these bands have been assigned to copper oxide-related vibrations. Similar spectral features due to $Cu_2O$ have been observed in the 400−600 $cm^{-1}$ region by IR[31] and Raman spectroscopy.[32] The broad peak around 400−435 $cm^{-1}$ of spectra obtained at −0.2 or −0.1 V in Figure 6, a or b, respectively, showed a slight frequency shift upon solution $H_2O/D_2O$ exchange, $\Delta = -8 \pm 5$ $cm^{-1}$ (data not shown), indicative of Cu−$OH^-$ vibration. Further support for this mode assignment was seen in experiments performed in solution I where, at potentials more negative than −0.40 V, a broad feature located at 448 $cm^{-1}$ emerged for which the frequency shift was more pronounced ($\Delta = -12 \pm 4$ $cm^{-1}$). The strength of this feature leads to the hypothesis that the absence of adsorbed phosphate peaks in solution I is due to hydroxide ion displacement in this very alkaline environment.

In summary, surface oxides and adsorbed hydroxide ions can effectively displace phosphate anions on Au and Cu electrodes. We did not observe similar phenomena on Ag electrodes.

**4.2. Spectra Interpretation: Phosphates.** The basis for interpreting our SER spectra of adsorbed phosphate anions include the relationship of these spectra to solution spectra of phosphate anions including the effects of solution $H_2O/D_2O$ isotopic exchange (Table 2 and refs 23 and 33), IR spectra of metal−phosphate complexes in aqueous solution,[34] and results of others showing effects of adsorption on vibrational spectra.[13−16,35,36] General features of our adsorbed phosphate anion vibrational spectra for Ag, Au, and Cu electrodes which suggest an influence of adsorption include (a) the increased number of bands observed in surface spectra relative to solution spectra, (b) the shift in frequencies of the surface spectra, (c) the broadening of the P−O stretching vibrations in the frequency region 800−1200 $cm^{-1}$ (Figures 2, 4, and 6; Table 2) relative to solution spectra,[22,23] and (d) the appearance of the low-frequency band at 230−320 $cm^{-1}$ (absent in the solution phosphate spectra) indicating the formation of the metal−anion bond.[6,8]

In the following sections, we identify the major adsorbed phosphate species, assign vibrational modes to the spectra peaks, and indicate probable orientation of phosphate anions on the surfaces of the various electrodes. Table 3 summarizes the assignments of the SERS bands. Frequency and intensity dependence of assigned phosphate bands on potential are shown in Figures 8 and 10, respectively.

*4.2.a. Adsorbed $PO_4^{3-}$ and $HPO_4^{2-}$ Ions.* Measurements of the vibrational bands of adsorbed $PO_4^{3-}$ ion were obtained from the spectra in solutions I and II, where solution concentration of $PO_4^{3-}$ species was in great excess over other phosphate species (Table 1). In the most alkaline solution I, we postulate that $PO_4^{3-}$ is the adsorbed species rather than $HPO_4^{2-}$ on the basis of its large solution excess, $[PO_4^{3-}]/[HPO_4^{2-}] = 33$, and because it has been previously shown that acidity of the bound species increases, relative to the bulk species, in studies of phosphate species adsorption to platinum[12] or complexation to cobalt ions.[34] This enhancement of surface acidity is due to the bonding of phosphate with the metal, thereby reducing the capacity for phosphate species to ligate hydrogen ions. Preferential adsorption of $SO_4^{2-}$ over $HSO_4^-$ species has also been demonstrated on Au electrodes.[37] The $[PO_4^{3-}]/[HPO_4^{2-}]$ ratio at the surface is also expected to increase relative to bulk solution for increasingly positive electrode potentials.[11,35,36]

In the less alkaline solution II, the $[PO_4^{3-}]/[HPO_4^{2-}]$ ratio is decreased from 33 to 7, relative to solution I. However, since the spectra obtained on the Ag electrode were so similar (Figure 3), we assume that $PO_4^{3-}$ is the dominant adsorbed species in both cases. For the Au and Cu electrodes, we also assume that $PO_4^{3-}$ is the dominant adsorbed species. The overwhelming strength of hydroxide ion features found in the SER spectra of solution I, caused by the strong $\nu$(M−OH) mode, and the extremely low intensity of the bands in the higher frequency region did not permit comparisons of phosphate-related features to be made between these two solutions.

In solution III, $[PO_4^{3-}]/[HPO_4^{2-}]$ is 0.004 so that the observed SER spectra are assumed to be dominated by $HPO_4^{2-}$ features. This is indicated for the Ag electrode by the differences in SER spectra observed in solution III (Figure 2a,b) where there are frequency upshifts for the 230−240 and 1070−1090 $cm^{-1}$ modes, as well as broadening of the bands in the region 900−1100 $cm^{-1}$. Comparison of spectra for solutions II−III on Au and Cu show similar tendencies as for the Ag electrode, and we assume that $HPO_4^{2-}$ is the dominant adsorbed species for these electrodes also.

**TABLE 3: Interpretation of the SER Spectra from Adsorbed Phosphate Anions on Ag, Au, and Cu Electrodes**

| Ag | | | Au | | | Cu | | | |
|---|---|---|---|---|---|---|---|---|---|
| *E*, V | freq, $cm^{-1}$ | Δ, $cm^{-1}$ | *E*, V | freq, $cm^{-1}$ | Δ, $cm^{-1}$ | *E*, V | freq, $cm^{-1}$ | Δ, $cm^{-1}$ | assignt |
| | | | | | $PO_4^{3-}$ | | | | |
| −0.20 | 230 | 3 ± 6 | 0.40 | 259 | | −0.60 | 302 | 3 ± 6 | $\nu$(M−O′) |
| −0.20 | 424 | 0 ± 5 | | | | | | | $\delta_s(PO_3)$ |
| −0.20 | 567 | 9 ± 3 | 0.40 | 570 | 15 ± 3 | −0.60 | 607 | 4 ± 4 | $\delta_{as}(PO_3)$ |
| −0.20 | 926 | −3 ± 2 | 0.40 | 918 | −1 ± 4 | −0.60 | 930 | −4 ± 2 | $\nu$(P−O′) |
| −0.20 | 1074 | −11 ± 2 | 0.40 | 1082 | −8 ± 3 | −0.60 | 1103 | −12 ± 3 | $\nu_{as}(PO_3)$ |
| | | | | | $HPO_4^{2-}$ | | | | |
| −0.20 | 241 | 3 ± 6 | 0.40 | 271 | 3 ± 6 | −0.60 | 319 | 5 ± 5 | $\nu$(M−O′) |
| −0.20 | 566 | 9 ± 3 | 0.40 | 574 | 15 ± 3 | | | | $\delta_{as}(PO_n)$ |
| −0.20 | 928 | −3 ± 2 | 0.40 | 923 | −3 ± 4 | −0.60 | 932 | −3 ± 2 | $\nu$(P−O′) |
| −0.20 | 1084 | −12 ± 2 | 0.40 | 1089 | −4 ± 3 | −0.60 | 1105 | −8 ± 3 | $\nu_{as}(PO_n)$ |
| | | | | | $H_2PO_4^-$ | | | | |
| | | | | | | −0.3 | 307 | 3 ± 4 | $\nu$(Cu−O′) |
| | | | | | | −0.3 | 907 | −11 ± 3 | $\nu$[P−$(OH)_2$] |
| | | | | | | −0.3 | 975 | 0 ± 3 | $\nu$(P−O′) |
| | | | | | $H_2P_2O_7^{2-}$ | | | | |
| | | | | | | −0.1 | 726 | 5 ± 3 | $\nu$(P−O−P) |
| | | | | | | −0.1 | 1021 | −2 ± 4 | $\nu$(P−O) |

[a] Abbreviations: $\Delta = \nu(D_2O) - \nu(H_2O)$ frequency shift upon solution $H_2O/D_2O$ exchange; $\nu$ = stretching vibration; $\delta$ = deformation vibration; as = asymmetric; s = symmetric; data for $PO_4^{3-}$ ion obtained from solution II, for $HPO_4^{2-}$ from solution III, and for $H_2PO_4^-$ ($H_2P_2O_7^{2-}$) from solution IV; $n$ = number of oxygen atoms that are exposed to solution and are hydrogen-bonded.

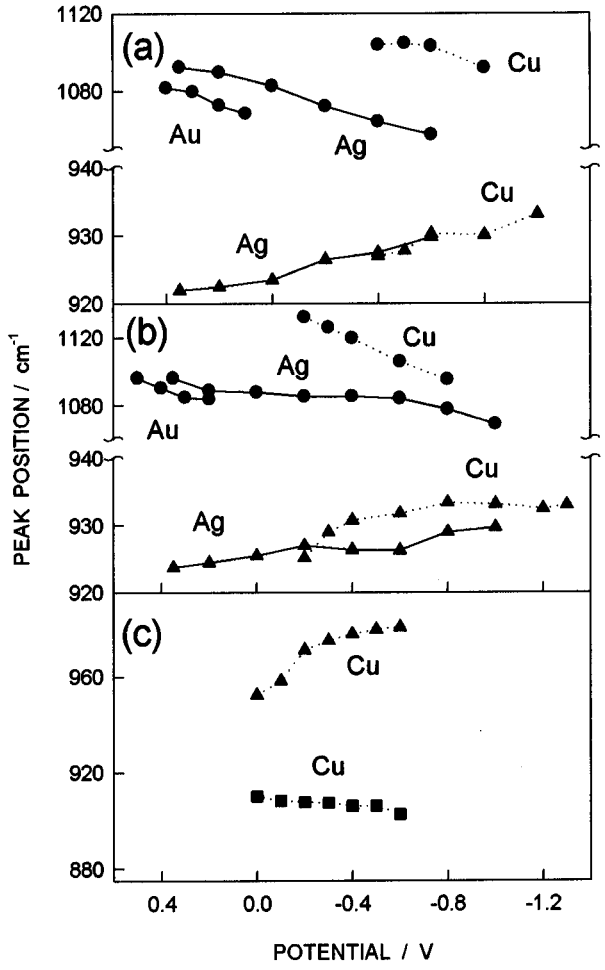


**Figure 8.** SERS peak position dependence on electrode potential for adsorbed phosphate species on Ag, Au, and Cu electrodes: (a) solution II (0.1 M NaOH + 0.067 M $Na_2HPO_4$); (b) solution III (0.067 M $Na_2HPO_4$); (c) solution IV (0.067 M $NaH_2PO_4$). Vibrational modes: (●) $\nu_{as}(PO_n)$; (▲) $\nu$(P−O′); (■) $\nu$[P−(OH)].

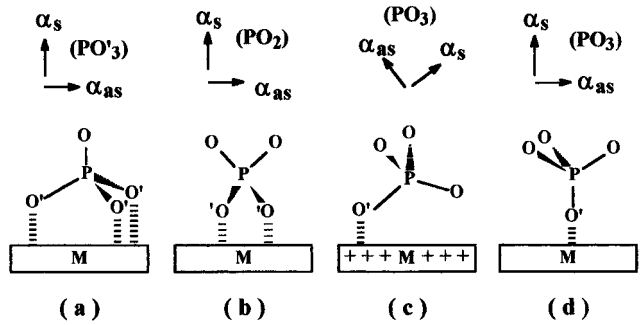


**Figure 9.** Possible adsorption geometries for $PO_4^{3-}$ anion on electrode surfaces. Coordination: (a) tridentate ($C_{3v}$ symmetry); (b) bidentate ($C_{2v}$ symmetry); (c) monodentate ($C_s$ symmetry); (d) monodentate ($C_{3v}$ symmetry). The main changes in the polarizability ellipsoid for symmetric and asymmetric stretching vibrations of the P−O and P−O′ bonds are shown by vector α. Oxygen atoms that interact with surface are denoted as O′.

It is interesting to note that differences in the spectra between adsorbed $PO_4^{3-}$ and $HPO_4^{2-}$ anions on the three electrodes are small compared to the differences between these two anionic species that are observed in solution spectra. This different spectral response between species in solution versus in the metal-adsorbed state may reflect diminished distinction between P−O−H···O and P−O···H−O bonding at the interface. Previous studies on the vibrational spectra of phosphates in solution and crystals have shown similar proton-transfer equilibria.[38,39] Also, partial charge transfer upon adsorption leading to decreased electrostatic repulsion[40,41] could be an additional reason that hydrogen bonding increases for adsorbed anions.

The vibrational mode assignments shown in Table 3 are made from spectra on Ag (Figure 2a), Au (Figure 4a), and Cu (Figure 6a) where the different metal electrodes were thought to be free of surface oxides and at similar charge (neutral or slightly positive). Previous investigators have considered assignments of specific vibrational modes to features of the SER spectra from phosphate anions adsorbed on silver colloids[9,10] or electrodes.[11] These studies do not provide a consensus about mode assignments, and none of them involved conditions that were completely equivalent to ours. Many of the differences among the interpretations derive from different assumptions made about the identity of phosphate species associated with the Ag surface and about the concentration relationship of phosphate species and hydrogen ions between bulk solution and metal surfaces. Unlike the previous assignments, ours rely

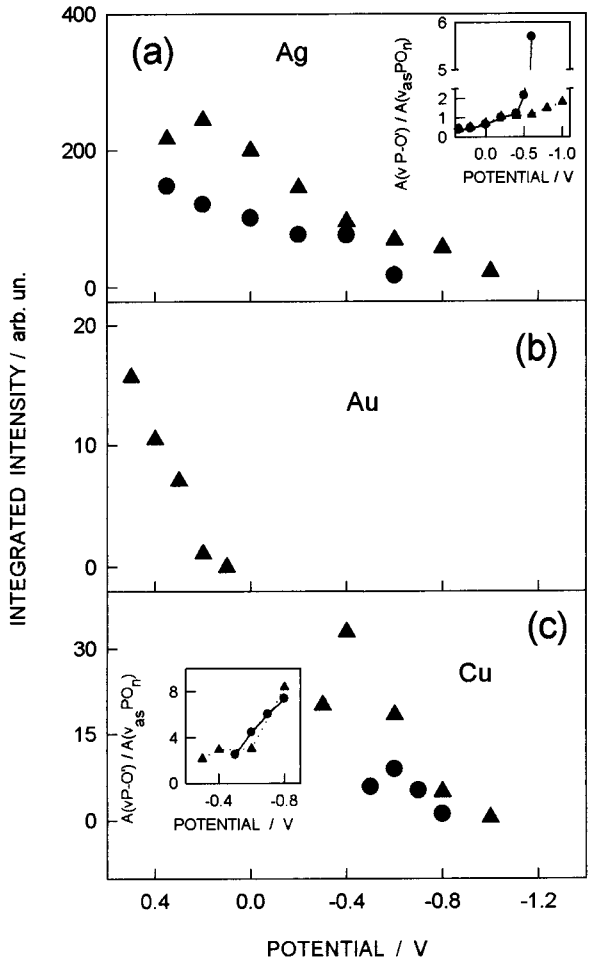


**Figure 10.** Comparison of the SERS integrated intensity vs potential dependence of the low-frequency mode $\nu$(M−O′) from the adsorbed phosphate species on Ag, Au, and Cu electrodes. Solutions: (●) solution II; (▲) solution III. Inserts show the dependence of the ratio of integrated intensities for the modes $\nu$(P−O′)/$\nu_{as}$(PO$_n$) on electrode potential.

heavily on the shifts of peak frequencies seen in our $H_2O/D_2O$ exchange experiments.

The highest frequency band located at 1070−1100 cm$^{-1}$ downshifted ∼6−10 cm$^{-1}$ when solution $H_2O$ was exchanged with $D_2O$, indicating that this mode is sensitive to hydrogen bonding and thus is related to the vibrations of the P−O bonds exposed to the solution. The Raman investigations of the $PO_4^{3-}$ ion in solution also showed that the asymmetric $\nu_{as}(PO_4)$ mode is sensitive to $H_2O/D_2O$ exchange and downshifted about 6 cm$^{-1}$ in $D_2O$ compared with $H_2O$ (Table 2). The symmetric $\nu_s(PO_4)$ mode was less sensitive to $H_2O/D_2O$ exchange. Therefore, we assign the highest frequency SER band to the $\nu_{as}(PO_n)$ mode of the adsorbed $PO_4^{3-}$ ion, where $n$ is the number of hydrogen-bonded oxygen atoms that are exposed to the solvent. We will show later, through consideration of possible adsorption geometries, that the most probable coordination takes place through one oxygen atom, and thus $n = 3$.

The band located at 920−930 cm$^{-1}$ is assigned to the stretching vibration of the P−O′ bond (where O′ denotes the oxygen atom bonded with the surface). This assignment is based on the high intensity of this band, its low sensitivity to $H_2O/D_2O$ exchange, and the frequency upshift as electrode potential was made more negative (Figure 8). A decrease of interaction strength with the surface is expected for adsorbed anions at more negative potentials,[41] which should lead to an increase in the P−O′ bond force constant and an increase in $\nu$(P−O′) frequency.[43,44] An alternative assignment of this band could be symmetric stretching vibration,[10] $\nu_s(PO_n)$; however, since the high-frequency band at 1070−1100 cm$^{-1}$ is more reliably assigned to the asymmetric stretching vibration (and this mode shifts to higher frequency region for adsorbed anions), the corresponding symmetric stretching mode should also be seen at elevated frequencies compared to solution (Tables 2 and 3). Such frequency shifts are in accord with the view that coordination with a metal surface decreases the double-bond character of the P−O′ bond. This causes an increase in bond length and a decrease in corresponding frequency. On the other hand, as double bonding between phosphate and solvent-exposed oxygen (P−O bonds) increases, there is a decrease in bond length and an increase in corresponding symmetric and asymmetric stretching frequencies. The best candidate for mode $\nu_s$ (PO$_n$) could be the not-clearly-resolved band around 940−950 cm$^{-1}$ (Figure 2). We suppose that at more negative potentials (−0.8 to −1.2 V), where interaction with the surface decreases, the difference between P−O′ and P−O bonds diminishes, and the $\nu$(P−O′) mode transforms to $\nu_s(PO_n)$, with a corresponding intense band in the spectra around 930 cm$^{-1}$ (Figures 2 and 6).

The band located at 565−610 cm$^{-1}$ is assigned to the $\delta_{as}(PO_n)$ vibration of the solvent-exposed P−O bonds due to its high sensitivity to $H_2O/D_2O$ exchange and to shifts to higher frequency in $D_2O$ solutions compared with $H_2O$ (Table 3). The same shift was observed for the $\delta_{as}(PO_4)$ mode in the solution Raman spectrum of the $PO_4^{3-}$ ion (Table 2). Siiman and Feilchenfeld[10] proposed this same assignment for a 575 cm$^{-1}$ band.

The low-frequency band located at 230−320 cm$^{-1}$ is far below the expected internal vibrational modes of adsorbed phosphate anions and thus is assigned to the stretching mode of a phosphate oxygen−metal bond, $\nu$(M−O′). These modes usually are observed as intense, broad bands in the SER spectra of chemisorbed species[6−8] and can be considered as the analogue of metal−ligand modes in coordinated compounds. In the case of phosphate−mercury(II) complexes, the phosphate oxygen−metal vibrational mode has been observed[45] at 269 cm$^{-1}$.

SER spectra above 500 cm$^{-1}$ of phosphate anions on Ag electrodes have also been reported by Dorian et al.[11] over a broad range of pH (0.8−13.4 pH units) and high electrolyte concentration (1 M total phosphate). At positive electrode potentials where Ag surface oxidation takes place, in all solutions except $H_3PO_4$, the adsorbed $PO_4^{3-}$ ion and insoluble $Ag_3PO_4$ were the predominant forms of surface phosphate. The Dorain et al. assignments at these conditions are 1079 cm$^{-1}$ [$\nu_{as}(PO_4)$], 910 cm$^{-1}$ [$\nu_s(PO_4)$], 555 cm$^{-1}$ [$\delta_{as}(PO_4)$], and 425 cm$^{-1}$ [$\delta_s(PO_4)$]. We found similar spectra (main peaks at 1049, 912, 566, and 436 cm$^{-1}$; data not shown) in alkaline solution at positive Ag electrode potentials where there was significant current flow. These bands showed no frequency shifts upon solution $H_2O/D_2O$ exchange and were therefore considered to be due to surface $Ag_3PO_4$ species where the oxygen atoms are coordinated with silver atoms (as opposed to adsorbed $PO_4^{3-}$ species where some oxygen atoms would be hydrogen-bonded with water and therefore sensitive to $H_2O/D_2O$ exchange). Formation of surface $Ag_3PO_4$ compounds at open-circuit conditions, as in the case of silver sols in phosphate solutions, could be one of the reasons that Greaves and Griffith[9] were unable to observe frequency shifts upon solution $H_2O/D_2O$ exchange. At more negative potentials, Dorain et al. assigned bands seen at 1070 and 570 cm$^{-1}$ to the $HPO_4^{2-}$ ion and the band at 925 cm$^{-1}$ to the adsorbed $H_2PO_4^-$ ion. Related SERS features have been interpreted differently.[9,10]

SER spectra also reveal information about the geometry and coordination of the $PO_4^{3-}$ ion at the metal electrode surfaces.

In aqueous solutions, the $PO_4^{3-}$ ion has tetrahedral symmetry, and all P−O bonds are equivalent.[22,23] Four bands were observed in the Raman spectrum, and the totally symmetric mode $\nu_s(PO_4)$ was dominant (Table 2). Upon coordination to a metal surface, the oxygen atoms become unequivalent, and consequently the degenerate modes split into separate distinguishable components. In general, three coordination types are possible, as shown in Figure 9: three oxygen atom−surface interactions (tridentate coordination, assuming $C_{3v}$ symmetry for $PO_4^{3-}$ ion); two oxygen atom−surface interactions (bidentate coordination, assuming $C_{2v}$ symmetry); and one oxygen atom−surface interaction (monodentate coordination, assuming either $C_s$ symmetry as shown in Figure 9c or $C_{3v}$ symmetry as in Figure 9d). These different coordination types can be recognized from the number of bands that appear in the complex spectra when phosphate ionic species ligate with metal ions in solution.[34] For example, monodentate coordination causes a split of the $\nu_3$ ($F_2$) mode into two modes, the symmetric stretch ($A_1$) and the double degenerate stretch (E), while bidentate coordination causes the split of the $\nu_3$ ($F_2$) mode into three modes, one symmetric stretch and two asymmetric stretch modes. However, for surface ligated species, the number of observed bands is not a sufficient indication of coordination type because surface selection rules influence band intensities—some vibrations could appear as very weak or even negligible intensity bands.[42] Finally, our analysis of $PO_4^{3-}$ ion coordination adopts the approach of Pemberton et al.[46] by assuming that the major changes in the polarizability ellipsoid for the $\nu_s(PO_3)$ mode occur in the direction of the P−O′ bond ($\alpha_s$ in Figure 9c,d), while major changes for the corresponding $\nu_{as}(PO_3)$ mode occur in the perpendicular direction ($\alpha_{as}$ in Figure 9c,d).

Tridentate coordination is readily ruled out since both the asymmetric stretching mode $\nu_{as}(PO_n)$ and the asymmetric deformation mode $\delta_{as}(PO_n)$ were found to be sensitive to $H_2O$/$D_2O$ exchange, indicative of solution-exposed P−O bonds that are hydrogen-bonded with solvent molecules. Bidentate coordination is ruled out because the intensity of these peaks (Figure 2a, 1074 and 567 $cm^{-1}$) is too strong to be consistent with the surface selection rule that asymmetric modes ($\alpha_{as}$ is parallel with respect to the surface in Figure 9b) in this adsorption geometry are very weak.[42] This leaves monodentate as the most probable coordination geometry. These structures can be stabilized by hydrogen-bonded water molecules; such interactions are clearly evidenced by results from the solution $H_2O$/$D_2O$ exchange experiments. This coordination geometry also provides a rationale for the experimental observations described in Figure 10, showing that the relative intensity of $\nu$(P−O′) compared with that of $\nu_{as}(PO_3)$ increases at more negative potentials (Figure 10, inserts). At more positive potentials, Figure 9c suggests that the asymmetric vibration has a component of the polarizability ellipsoid that is perpendicular to the surface and therefore should display the high-intensity asymmetric stretching mode that was seen for the 1091−1074 $cm^{-1}$ peak of Figure 2a. The decrease in relative intensity of this peak with decreasing potential can be rationalized by migration of the $PO_3$ group away from the surface as the potential becomes more negative, as shown in Figure 9d. In this model, the intensity of the $\nu$(P−O′) mode increases with decreasing potential (see 922−926 $cm^{-1}$ peak, Figure 2a) because the main changes in the polarizability ellipsoid related to this vibration occur in the direction perpendicular to the surface. These simultaneous, opposing trends are illustrated by the inserts of Figure 10 which show that the measured intensity ratio, $A[\nu(P-O')]/A[\nu_{as}(PO_n)]$, increases with declining potential.

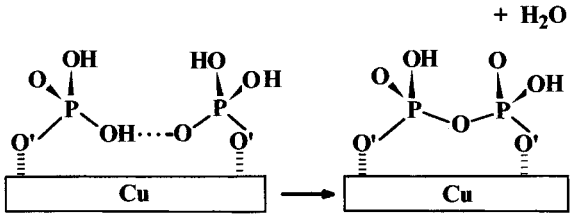


**Figure 11.** Possible mechanism for formation of P−O−P bond in acidic solutions on Cu electrodes. Oxygen atoms that interact with surface are denoted as O′.

Since observed spectral patterns in solutions II and III are similar, and since no high-frequency bands could be assigned to metal−hydrogen bonds in our spectra, we do not think coordination of $HPO_4^{2-}$ species will be substantially different from that of $PO_4^{3-}$. Only the stretching vibration frequencies would be affected (increased), as suggested by comparisons of spectra for solution II and solution III (Figure 3).

*4.2.b. Adsorbed $H_2PO_4^-$ Ion.* Adsorbed $H_2PO_4^-$ ions were seen clearly only in the spectra obtained on Cu electrodes immersed in solution IV (Figure 6c and Figure 7) or solution V (Figure 6d and Figure 7). The similarity of the spectra from both solutions suggests that they are due to the same major adsorbed species. The main band that we relate with the adsorbed $H_2PO_4^-$ ion is the intense peak at 908−910 $cm^{-1}$ observed in both solution IV and V at relatively positive potentials (Figure 6c,d). This band downshifts by 11−15 $cm^{-1}$ in $D_2O$ solutions (Figure 7). In addition, the fwhm of this band increases from 30 $cm^{-1}$ in $H_2O$ to 45 $cm^{-1}$ in $D_2O$ solution (Figure 7). Exactly the same tendency was observed for $H_2PO_4^-$ ions in solution spectra (Table 2). This 907 $cm^{-1}$ band is assigned to the P−OH bond stretching mode of the symmetric P−$(OH)_2$ vibration. The higher frequency of this mode (907 $cm^{-1}$ at $E = -0.30$ V) compared with $H_2PO_4^-$ ion in solution (877 $cm^{-1}$, Table 2) indicates strong hydrogen bonding between adsorbed species as depicted in Figure 11. An increase in P−OH vibration frequency was also observed for $H_2PO_4^-$ ions adsorbed on Pt.[36] The enhanced interaction between neighboring adsorbed dihydrogen phosphate anions relative to adsorbed $PO_4^{3-}$ or $HPO_4^{2-}$ ions is promoted by a decrease in ionic charge due to the protonation. It is also noteworthy that the frequency of the $\nu_s$[P−$(OH)_2$] mode decreases at more negative potentials (Figure 6c,d), suggesting that strength of hydrogen bonding is decreased.

Another band that we attribute to adsorbed $H_2PO_4^-$ ion is the partially resolved peak at around 975−980 $cm^{-1}$. This band is assigned to the stretching vibration of the P−O′ bond. The frequency of this mode is lower than that of the $\nu_s(PO_2)$ mode observed for the solution $H_2PO_4^-$ species (1077 $cm^{-1}$, see Table 2) due to decreased double-bond character of the P−O′ bond when there is coordination with the surface through the O′ atom. The frequency of this mode upshifted at more negative potentials (Figure 6c,d), reflecting diminished interaction with the surface. Finally, the third band related with adsorbed $H_2PO_4^-$ ion is the broad, low-frequency peak located at ∼307 $cm^{-1}$ (Figure 6c). As per reasons discussed previously for other low-frequency peaks in solutions with adsorbing species, this band is assigned to the stretching vibration of the metal−anion bond, $\nu$(Cu−O′).

The adsorbed diphosphate species, $H_2P_2O_7^{2-}$, is identified in the SER spectra obtained on Cu electrodes on the basis of the spectral feature seen around 724−731 $cm^{-1}$ in Figure 6c,d. The relative intensity of this mode was higher in the more acidic solution V. This band showed only a slight frequency shift in the solution $H_2O$/$D_2O$ exchange experiments. While this band

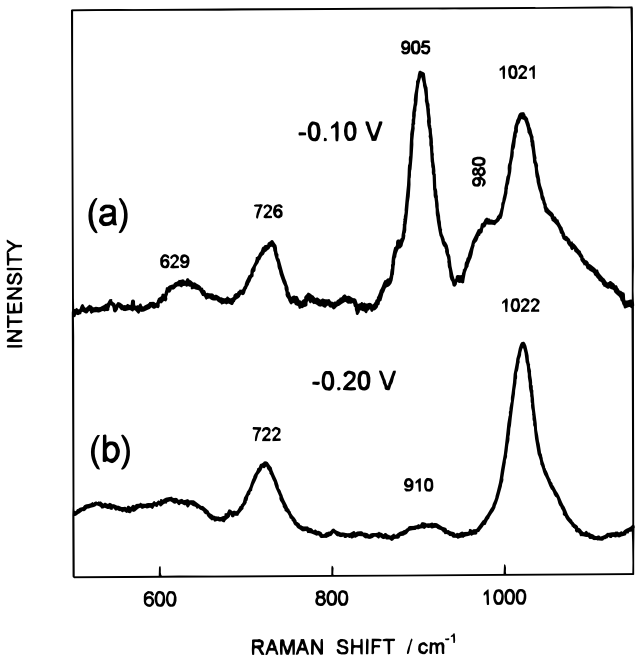


**Figure 12.** SER spectra from a Cu electrode: (a) solution V (0.1 M $HClO_4$ + 0.067 M $NaH_2PO_4$) at $E = -0.1$ V; (b) 0.067 M $Na_2H_2P_2O_7$ at (pH 7.7) and $E = -0.2$ V.

has not been previously observed in solution spectra of phosphate anions or $H_3PO_4$,[22,23] bands in the region 700−750 $cm^{-1}$ are characteristic for diphosphate anion.[33] Figure 11 depicts a possible explanation for the origin of this band due to formation of a P−O−P bond between neighboring adsorbed $H_2PO_4^-$ ions according to the reaction

$$[H_2PO_4^-]_{ad} + [H_2PO_4^-]_{ad} = [H_2P_2O_7^{2-}]_{ad} + H_2O \quad (1)$$

Support for this suggestion comes from a comparison of SER spectra for Cu electrodes immersed in solution V with a spectrum for the same electrode immersed in an authentic diphosphate anion solution (0.067 M $Na_2H_2P_2O_7$, adjusted to pH 7.7 with NaOH). The comparison shown in Figure 12 suggests that the characteristic frequency for the P−O−P bridge vibration[33] at 722 $cm^{-1}$ in the authentic diphosphate spectrum is the origin of the 726 $cm^{-1}$ band observed in the acidic phosphate solution V. No (or very little) frequency shift was observed for this band upon solution $H_2O/D_2O$ exchange. Another band located at ∼1022 $cm^{-1}$ was observed in both spectra and is assigned to the stretching vibration $\nu$(P−O) of the surface diphosphate anion. The symmetric stretching vibration at around 1020 $cm^{-1}$ usually is observed as the most intense band in the solutions containing diphosphate anion.[33]

A possible adsorption geometry for the $H_2PO_4^-$ anion on the Cu electrode, along with a proposed mechanism for formation of the adsorbed $H_2P_2O_7^{2-}$ species, is shown in Figure 11. The presence of the strong, broad mode at 307 $cm^{-1}$, which showed no sensitivity to solution $H_2O/D_2O$ exchange, suggests the same monodentate coordination with the copper surface that was postulated earlier for $PO_4^{3-}$ ion coordination through the oxygen atom O′. If the coordination were bidentate, a considerably lower frequency for the $\nu$(Cu−O′) mode should have been observed.[47] Simultaneous peaks associated with the $\nu$(Cu−O′) mode (307 $cm^{-1}$) and the $\nu$(P−O′) mode (975 $cm^{-1}$) are most readily seen in the spectrum for solution IV at an electrode potential of −0.3 V (Figure 6c). The reason for postulating a relatively high angle between the P−O′ bond and the surface normal shown in Figure 11 is due to the low intensity that was observed for the $\nu$(P−O′) mode. The P−OH bonds are shown to be hydrogen-bonded, as was discussed earlier.

**4.3. Comparison of the Ag, Au, and Cu Electrodes.** The potential window where specifically adsorbed phosphate species are observed depends on the nature of the electrode. In Figure 10, we compare the potential range where phosphate adsorption occurred on three metal electrodes. In this figure, the integrated intensity of the phosphate oxygen−metal bond stretch, $\nu$(M−O′), is shown as a function of imposed electrode potential. This SER signal intensity is taken as a rough indication of degree of phosphate anion adsorption on the basis that it is relatively insensitive to adsorbate ion orientation. The general tendency was a decrease in adsorption as potential becomes more negative. For the Ag and Cu electrodes, the SER intensity (and presumably the amount of adsorbed phosphate) also was observed to decline as potentials become more positive relative to the intensity maxima potentials. In this case, there is thought to be increasing competition from $OH^-$ ions for surface adsorption sites.

One of the important properties of the interface affecting anion adsorption is its potential of the zero charge (pzc).[48,49] This is especially critical for the highly negative phosphate anions. There is relative agreement in the literature concerning the values for the pzc of polycrystalline gold and silver.[50−52] In surface-inactive electrolytes, the pzc of the Au electrode is about 0.2−0.3 V, while for the Ag electrode it is ∼−0.7 V. When specific adsorption of anions takes place, the pzc shifts to more negative values.[48,49] The potential range for phosphate adsorption on Ag was about 1 V more negative than for adsorption on Au. This is comparable with the difference in pzc for these two electrodes. In the case of the Cu electrode, adsorbed phosphate species were observed until potentials more negative than about −0.7 to −1.0 V were reached. This indicates that the pzc of the Cu electrodes in phosphate solutions should be in the rather negative potential range. Comparing these results with interpretation of previous measurements of the pzc of Cu electrodes by others is complicated due to the high affinity of copper to form oxides.[53] We favor measurements that used in situ surface abrasion techniques that tended to minimize the influence of copper oxides.[51,53,54] In these cases, the pzc of polycrystalline copper in solutions of nonadsorbing electrolytes has been established to be in the range −0.35 to −0.88 V (vs SHE). Specific adsorption of phosphate anions should cause shifts of the pzc toward the more negative potentials that were observed in our spectroscopic results.

The relative strength of the metal−oxygen bond for the three electrode materials can be analyzed in terms of the asymmetric stretching frequencies of the internal phosphate vibration, $\nu_{as}(PO_n)$, and more directly in terms of the M−O′ bond force constants. The sensitivity of the $\nu_{as}(PO_n)$ mode to the nature of electrode material was seen as downshifted frequencies (Table 3) for the progression Ag (1074 $cm^{-1}$) to Au (1082 $cm^{-1}$) to Cu (1103 $cm^{-1}$) and again as Ag (1084 $cm^{-1}$) to Au (1089 $cm^{-1}$) to Cu (1105 $cm^{-1}$). The considerably higher frequency of this mode in the case of adsorbed $PO_4^{3-}$ compared with the frequency in solution (1013 $cm^{-1}$ from Table 2) can be explained by an increase in $\pi$ bonding between P and non-coordinated O atoms upon adsorption. This suggests that as the interaction with the surface becomes stronger, the $\pi$-bonding of the P−O′ bond decreases, while the $\pi$-bonding for P−O bonds increases, causing shortening of the P−O bonds and an increase in $\nu_{as}(PO_n)$ frequency. Comparison of $\nu_{as}(PO_n)$ frequencies for the different electrodes, at potentials close to those that give positive surface charges on all electrodes, showed the following order:

**TABLE 4: Raman Frequencies ($\nu$) and Force Constants ($k$) for Metal−Oxygen Bonds of Adsorbed Phosphate Anions at Electrode Surfaces[a]**

| electrode | solution | $E$, V | ion | mode | $\nu$, cm$^{-1}$ | $k$, mdyn Å$^{-1}$ |
|---|---|---|---|---|---|---|
| Ag | II | −0.20 | $PO_4^{3-}$ | $\nu$(Ag−O′) | 230 | 0.43 |
| Ag | III | −0.20 | $HPO_4^{2-}$ | $\nu$(Ag−O′) | 242 | 0.48 |
| Ag | III | −0.90 | $HPO_4^{2-}$ | $\nu$(Ag−O′) | 239 | 0.47 |
| Au | II | 0.40 | $PO_4^{3-}$ | $\nu$(Au−O′) | 259 | 0.59 |
| Au | II | 0.20 | $PO_4^{3-}$ | $\nu$(Au−O′) | 249 | 0.54 |
| Au | III | 0.60 | $HPO_4^{2-}$ | $\nu$(Au−O′) | 271 | 0.64 |
| Au | III | 0.40 | $HPO_4^{2-}$ | $\nu$(Au−O′) | 256 | 0.57 |
| Cu | II | −0.60 | $PO_4^{3-}$ | $\nu$(Cu−O′) | 301 | 0.68 |
| Cu | III | −0.60 | $HPO_4^{2-}$ | $\nu$(Cu−O′) | 320 | 0.77 |
| Cu | IV | 0.00 | $H_2PO_4^-$ | $\nu$(Cu−O′) | 307 | 0.71 |

[a] Force constants obtained from experimental SERS frequencies by using two atomic species approximation formula $k = 4\pi^2c^2\nu^2\mu$, where $c$ is the velocity of light and $\mu$ is the reduced mass of the metal and oxygen atoms.

$$\nu_{as}[PO_3\ (Cu)] > \nu_{as}[PO_3\ (Au)] \geq \nu_{as}[PO_3\ (Ag)]$$

This may indicate more covalent bonding character between the O′ atom and Cu, compared to either Ag or Au.

The bonding strength of the phosphate anions on the different electrode materials is most directly compared in terms of the M−O′ bond force constants. These force constants are correlated with bond length and describe bond strength between atoms at small distortions in bond length from the equilibrium distance.[55] Table 4 is a summary of force constants estimated from the measured $\nu$(M−O′) frequencies at different conditions. The metal surface mass was approximated by atomic mass, based in part on the success of this approximation in describing results from a study of $Cl^-$ adsorption on Cu electrodes,[19] where the isotopic $^{65}Cu/^{63}Cu$ frequency shift of the $\nu$(Cu−Cl) mode was observed, indicating that single Cu atoms rather than arrays of Cu atoms were involved in anion bonding. These force constant estimates also neglect effects of P−O internal modes on the M−O′ vibrations. Despite these simplifications, the trends shown in Table 4 show that the force constants are highest for Cu−O′ bonds and decrease in the following order: $k$(Cu−O′) > $k$(Au−O′) > $k$(Ag−O′). Also, for all three electrodes, the force constants are highest for adsorbed $HPO_4^{2-}$ ion.

## 5. Conclusions

SER spectra from adsorbed phosphate anions on Ag, Au, and Cu electrodes have been obtained in solutions prepared with $H_2O$ and $D_2O$. The highest frequency mode located at 1070−1110 cm$^{-1}$ was assigned to the asymmetric vibrational mode of the internal P−O bonds (non-surface-coordinated oxygen atoms). This mode showed high sensitivity to the environment through (a) a frequency downshift upon solution $H_2O/D_2O$ exchange, (b) a relatively high sensitivity to imposed electrode potential, and (c) a relatively high sensitivity to electrode material. The corresponding deformation asymmetric mode was assigned to the band located at ∼570 cm$^{-1}$. The frequency of this mode upshifted in $D_2O$ solutions compared to $H_2O$ solutions.

Monodentate surface coordination of the $PO_4^{3-}$ and $HPO_4^{2-}$ ions has been proposed. The dependence of the relative intensity of the internal modes on electrode potential was interpreted in terms of the migration of free ($PO_n$) groups from the surface at more negative potentials. In the case of the Au electrode, the non-surface-coordinated $PO_n$ group remained close to the surface at all potentials.

No spectroscopic evidence for chemisorption of the $H_2PO_4^-$ ion on Ag or Au electrodes was observed, contrary to the observations of $H_2PO_4^-$ ion adsorption on Cu electrodes. The adsorbed $H_2PO_4^-$ ion on Cu showed an intense band at ∼907 cm$^{-1}$, which decreased in frequency and broadened in $D_2O$ solutions, and was assigned to the stretching mode of the P−OH groups. In acidic solutions, formation of P−O−P bonds was observed on Cu electrodes, possibly as a result of strong interactions between pairs of adsorbed $H_2PO_4^-$ ions.

In the potential and pH ranges investigated, hydroxide ions were found to compete with phosphate species for adsorption sites on Au and Cu electrodes. After reduction of Au surface oxides, active sites are thought to be created, and adsorption of phosphate anions on these sites caused an increase in SERS signal intensity.

Force constants, derived from measured metal−oxygen frequencies, were compared for different electrodes, and the established bond strength was $k$(Cu−O′) > $k$(Au−O′) > $k$(Ag−O′).

## References and Notes

(1) Van Dulm, P.; Norde, W.; Lyklema, J. *J. Colloid Interface Sci.* **1981**, *82*, 77.
(2) Rospendovski, B. N.; Schlegel, V. L.; Holt, R. E.; Cotton, T. M. In *Charge and Field Effects in Biosystems-2*; Allen, M. J., Cleary, S. F., Hawkridge, F. M., Eds.; Plenum Press: New York, 1989; p 43.
(3) Daido, T.; Akaike, T. *J. Electroanal. Chem.* **1993**, *344*, 91.
(4) Lu, T.; Yu, X.; Dong, S.; Zhou, C.; Ye, S.; Cotton, T. M. *J. Electroanal. Chem*. **1994**, *369*, 79.
(5) Niaura, G.; Gaigalas, A. K.; Vilker, V. L. *J. Electroanal. Chem.* **1996**, *416*, 167.
(6) Chang, R. K. *Ber. Bunsen-Ges. Phys. Chem.* **1987**, *91*, 296.
(7) Pemberton, J. E. In *Electrochemical Interfaces: Modern Techniques for In-situ Interface Characterization*; Abruna, H. D., Ed.; VCH: New York, 1991; Chapter 5.
(8) Gao, P.; Weaver, M. J. *J. Phys. Chem.* **1986**, *90*, 4057.
(9) Greaves, S. J.; Griffith, P. *J. Raman Spectrosc.* **1988**, *19*, 503.
(10) Siiman, O.; Feilchenfeld, H. *J. Phys. Chem.* **1988**, *92*, 453.
(11) Dorain, P. B.; Von Raben, K. U.; Chang, R. K. *Surf. Sci.* **1984**, *148*, 439.
(12) Paulissen, V. B.; Korzeniewski, C. *J. Electroanal. Chem.* **1990**, *290*, 181.
(13) Iwasita, T.; Nart, F. C.; Polligkeit, H. *Ber. Bunsen-Ges. Phys. Chem.* **1991**, *95*, 638.
(14) Ye, S.; Kita, H.; Aramata, A. *J. Electroanal. Chem.* **1992**, *333*, 299.
(15) Nart, F. C.; Iwasita, T.; Weber, M. *Ber. Bunsen-Ges. Phys. Chem.* **1993**, *97*, 737.
(16) Weber, M.; Nart, F. C. *Electrochim. Acta* **1996**, *41*, 653.
(17) Certain commercial equipment, instruments, and materials are identified in this paper to specify adequately the experimental procedure. In no case does such identification imply recommendation of endorsement by the National Institute of Standards and Technology, nor does it imply that the material or equipment is necessarily the best available for the purpose.
(18) Gao, P.; Patterson, M. L.; Tadayyoni, M. A.; Weaver, M. J. *Langmuir* **1985**, *1*, 172.
(19) Niaura, G.; Malinauskas, A. *Chem. Phys. Lett.* **1993**, *207*, 455.
(20) *Lange's Handbook of Chemistry*, 13th ed.; Dean, J. A., Ed.; McGraw-Hill: New York, 1985; p 5-15.
(21) Horvath, A. L. *Handbook of Aqueous Electrolyte Solutions: Physical Properties, Estimation and Correlation Methods*; John Wiley: New York, 1985; p 212.
(22) Chapman, A. C.; Thirlwell, L. E. *Spectrochim. Acta* **1964**, *20*, 937.
(23) Preston, C. M.; Adams, W. A. *J. Phys. Chem.* **1979**, *83*, 814.
(24) Nakamoto, K. *Infrared and Raman Spectra of Inorganic and Coordination Compounds*, 4th ed.; John Wiley: New York, 1986; Chapters 2 and 3.
(25) Ashworth, V.; Fairhurst, D. *J. Electrochem. Soc.* **1977**, *124*, 506.
(26) Droog, J. M. M.; Alderliesten, C. A.; Alderliesten, P. T.; Bootsma, G. A. *J. Electroanal. Chem.* **1980**, *111*, 61.
(27) Gennero De Chialvo, M. R.; Zerbino, J. O.; Marchiano, S. L.; Arvia, A. J. *J. Appl. Electrochem.* **1986**, *16*, 517.
(28) Martel, A.; Cheong, A. K.; Lessard, J.; Brossard, L. *Can. J. Chem.* **1994**, *72*, 2353.
(29) Desilvestro, J.; Weaver, M. J. *J. Electroanal. Chem.* **1986**, *209*, 377.

(30) Pireaux, J. J.; Liehr, M.; Thiry, P. A.; Delrue, J. P.; Caudano, R. *Surf. Sci.* **1984**, *141*, 221.
(31) McDevitt, N. T.; Baun, W. L. *Spectrochim. Acta* **1964**, *20*, 799.
(32) Melendres, C. A.; Xu, S.; Tani, B. *J. Electroanal. Chem.* **1984**, *162*, 343.
(33) Eysel, H. H.; Lim, K. T. *J. Raman. Spectrosc.* **1988**, *19*, 535.
(34) Lincoln, S. F.; Stranks, D. R. *Aust. J. Chem.* **1968**, *21*, 37.
(35) Nart, F. C.; Iwasita, T. *J. Electroanal. Chem.* **1992**, *322*, 289.
(36) Nart, F. C.; Iwasita, T. *Electrochim. Acta* **1992**, *37*, 385.
(37) Shi, Z.; Lipkowski, J.; Gamboa, M.; Zelenay, P.; Wieckowski, A. *J. Electroanal. Chem*. **1994**, *366*, 317.
(38) Van Der Veken, B. J.; Herman, M. A. *J. Mol. Struct.* **1973**, *15*, 225.
(39) Jayakumar, V. S.; Rajagopal, P.; Aruldhas, G. *J. Raman Spectrosc.* **1991**, *22*, 593.
(40) Lorenz, W.; Sakie, G. *J. Electroanal. Chem.* **1977**, *80*, 1.
(41) Habib, M. A.; Bockris, J. O'M. In *Comprehensive Treatise of Electrochemistry*; Bockris, J. O'M., Conway, B. E., Yeager, E., Eds.; Plenum Press: New York, 1980; Vol. 1., Chapter 4.
(42) Creighton, J. A. In *Spectroscopy of Surfaces*; Clark, R. J. H., Hester, R. E., Eds.; Wiley: New York, 1988; Chapter 2.
(43) Cruickshank, D. W. J.; Robinson, E. A. *Spectrochim. Acta* **1966**, *22*, 555.
(44) Chapman, A. C.; Long, D. A.; Jones, D. T. L. *Spectrochim. Acta* **1965**, *21*, 633.
(45) Russell, S. J.; Tan, K.-H.; Taylor, M. J. *J. Raman Spectrosc.* **1980**, *9*, 308.
(46) Pemberton, J. E.; Brayant, M. A.; Sobocinski, R. L.; Joa, S. L. *J. Phys. Chem.* **1992**, *96*, 3776.
(47) Ferraro, J. R. *Low-Frequency Vibrations of Inorganic and Coordination Compounds*; Plenum: New York, 1971; Chapters 6 and 7.
(48) Bockris, J. O'M.; Reddy, A. K. N. *Modern Electrochemistry*; Plenum: New York, 1970; Vol. 2, Chapter 7.
(49) Frumkin, A. N.; Petrii, O. A.; Damaskin, B. B. In *Comprehensive Treatise of Electrochemistry*; Bockris, J. O'M., Conway, B. E., Yeager, E., Eds.; Plenum Press: New York, 1980; Vol. 1, Chapter 5.
(50) Trasatti, S. In *Advances in Electrochemistry and Electrochemical Engineering;* Gerischer, H., Tobias, Ch. W., Eds.; John Wiley: New York, 1977; Vol. 10, p 274.
(51) Clark, G. J.; Andersen, T. N.; Valentine, R S.; Eyring, H. *J. Electrochem. Soc*. **1974**, *121*, 618.
(52) Sokolowski, J.; Czajkowski, J. M.; Turowska, M. *Electrochim. Acta* **1990**, *35*, 1393.
(53) Henning, H.; Batrakov, V. *Elektrokhimiya* **1979**, *15*, 1833.
(54) Lasarova, E.; Nikolov, C. *Elektrokhimiya* **1986**, *22*, 1217.
(55) *Infrared and Raman Spectroscopy*; Schrader, B., Ed.; VCH: Weinheim, 1995; Chapter 4.